A Hilbert Curve Based Representation of sEMG Signals for the Problem of Gesture Recognition

Panagiotis Tsinganos [1,2], Bruno Cornelis [2], Jan Cornelis [2], Bart Jansen [2,3], Athanassios Skodras [1]
[1] University of Patras, Department of Electrical and Computer Engineering, 26504 Patras, Greece
[2] Vrije Universiteit Brussel, Department of Electronics and Informatics, 1050 Brussels, Belgium
[3] imec, 3001 Leuven, Belgium
{panagiotis.tsinganos, skodras}@ece.upatras.gr, {bcorneli, jpcornel, bjansen}@etrovub.be

***Abstract* – Deep learning (DL) has transformed the field of data analysis by dramatically improving the state of the art in various classification and prediction tasks especially in the area of computer vision. In biomedical engineering, a lot of new work is directed towards surface electromyography (sEMG) based gesture recognition addressed as an image classification problem using Convolutional Neural Networks (CNN). In this paper, we utilize the Hilbert space filling curve for the generation of image representations of sEMG signals that can be classified by a CNN. The proposed method is evaluated on different network architectures and yields a classification improvement of more than 3%.**

***Keywords* – Hilbert curve, hand gesture recognition, sEMG, electromyography, classification, CNN**

I. INTRODUCTION

The problem of gesture recognition is encountered in many applications including human computer interaction [29], sign language recognition [8], prosthesis control [7] and rehabilitation gaming [6, 27]. Signals generated from the electrical activity of the forearm muscles, which can be recorded with surface electromyography (sEMG) sensors, contain useful information for decoding muscle activity and hand motion [13].

Machine Learning (ML) classifiers have been used extensively for determining the type of hand motion from sEMG data. A complete pattern recognition system based on ML consists of data acquisition, feature extraction, classifier definition and inference from new data. For the classification of gestures from sEMG data, electrodes attached to the arm and/or forearm acquire the sEMG signals, and features such as RMS, variance, zero crossings and frequency coefficients are extracted and then applied as inputs to classifiers like k-NN, SVM, MLP and Random Forests [30].

Over the past years, Deep Learning (DL) models have shown great success to the problem of sEMG-based gesture recognition. In these approaches, EMG data are represented as images and a Convolutional Neural Network (CNN) is used to determine the type of gesture. A typical CNN architecture consists of a stack of convolutional and pooling layers followed by fully connected layers (dense) and a softmax output. In this way, CNNs transform the input image layer by layer from the pixel values to the final classification label.

CNNs have made breakthroughs in feature extraction and image classification tasks in 2D. Yet, choosing a method to convert time-series into images that can be used as inputs to CNN models is not obvious. Among the methods proposed in literature are the segmentation of multi-channeled signals using windows and the application of 2D transformations such as the Fourier and Wavelet Transforms.

In this work, we investigate the application of the Hilbert space filling curve to represent sEMG signals as images that can be classified by CNNs. This curve is useful because it provides a mapping between 1D and d-dimensional spaces that preserves locality. The main contributions presented in this paper are:

- the development of a method of representing sEMG signals as images using the Hilbert curve,
- the application of this method to the problem of hand gesture recognition with CNNs.

The paper is organized as follows. Section 2 provides an overview of the related gesture recognition approaches. In Section 3, we give a detailed description of the proposed method and the CNN architectures used for experimentation. The experiments performed for the evaluation of the model are presented in Section 4, while the results and a discussion are given in Section 5. Finally, Section 6 describes the conclusions and outlines future work.

II. RELATED WORK

The problem of sEMG-based hand gesture recognition has been studied thoroughly using either conventional ML techniques or DL methods. In the case of ML-based methods, the first significant study is presented in [18] for the classification of four hand gestures using time-domain features extracted from sEMG measured with two electrodes. The authors of [5] achieve a 97% accuracy in the classification of three grasp motions using the RMS value from seven electrodes as the input to an SVM classifier. The works of [23, 2, 15] evaluate a wide range of EMG features with various classifiers for the recognition of 52 gestures (Ninapro dataset [2, 1]). The best performance is observed with a combination of features and a Random Forest classifier resulting in 75% accuracy.

On the other hand, the first DL-based architecture, was proposed in [28]. The authors built a CNN-based model for the classification of six common hand movements resulting in a better classification accuracy compared to SVM. In [3], a

simple model consisting of five blocks of convolutional and average pooling layers resulted in accuracy figures comparable, though not higher, to what was obtained with classical ML methods. In our previous work [34], we have investigated methods to improve the performance of this basic model. The results have shown that opting for max pooling and inserting dropout [32] layers after the convolutions boosts the accuracy by 3% (from 67% to 70%). The works of [14, 37] incorporate dropout and batch normalization [20] techniques in their methodology. Apart from differences in model architectures, they measure EMG signals using a high-density electrode array, which has been proven effective to myoelectric control problems [21, 26, 33]. Using instantaneous EMG images, [14] achieves 89% accuracy on a set of eight movements, whereas in [37] a multi-stream CNN architecture is employed resulting in 85% accuracy on the Ninapro dataset.

Other important works based on DL architectures deal with the problem of model adaptation. In [12], the technique of adaptive batch normalization (AdaBN) [24] updates only the normalization parameters of a pretrained model, whereas in [10] the authors use weighted connections between a source network and the model instantiated for a new subject. Additionally, in [10] they propose data augmentation methods for sEMG signals.

The properties of the Hilbert curve have been utilized in previous works. In [11] and [22], mammographic images are represented as 1D vectors through the Hilbert curve and a combination of features is helpful in detecting breast cancer. The work of [9] follows a similar dimensionality reduction approach in mapping 3D data into 2D and 1D representations which are used by CNNs in order to classify 3D structural data. Compared to processing the raw 3D data directly, this method allows for reduced training time and increased number of data channels. In [4] the performance of LSTM-based model in the detection of image forgeries depends on the sequence of the extracted image patches. Therefore, to better preserve spatial locality, the Hilbert curve is employed to determine the order of image patches fed into the LSTM. Apart from applications in dimensionality reduction, the Hilbert curve has been successful in the inverse problem as well, i.e. representing 1D data as 2D images. In the work of [38] that deals with the problem of DNA sequence classification, the long-term interactions between regions of the sequence are important for the DNA classification. Instead of using very deep networks or larger filters, they utilize the Hilbert curve to map the DNA sequence into an image such that proximal elements stay close, while the distance between distal elements is reduced.

III. METHODS

A. Hilbert curve

A Hilbert curve (also known as a Hilbert space-filling curve) is a continuous fractal space-filling curve, i.e. a curve that traverses sequentially all the points of a d-dimensional space, that was first described by the German mathematician David Hilbert in 1891. Space filling curves have been widely applied to tasks in data organization and compression. Between the available curves, the Hilbert curve is known for being superior in preserving locality compared to alternative curves [25, 16].

The Hilbert curve can be constructed in a recursive manner. Initially, the 2D plane is divided into four quadrants that are traversed according to a fundamental pattern as shown in Fig. 1-a. From each iteration to the next, all existing subsquares are subdivided into four smaller subsquares. These four subsquares are connected by a pattern that is obtained by rotation and/or reflection of the fundamental pattern. Fig. 1 visualizes Hilbert curve traversals of the 2D space after the first iterations, where the numbers correspond to the index within the sequence that is mapped to the specific pixel.

B. sEMG representation

In this work, the Hilbert curve is employed to transform multi-channel sEMG signals into 2D image representations. Firstly, the sEMG data of a hand gesture recorded by K electrodes are organized into small segments of length N. Therefore, the dimensions of the data are N x K. Then, the mapping can be used in two ways: 1) across the time dimension, i.e. for each sEMG channel, map the time sequence into a 2D image, and 2) across the sEMG channels dimension, i.e. for each time instant, map the values of the channels into a 2D image. Examples of these representation are shown in Fig. 2.

The application of the Hilbert mapping across the time dimension, consists of the following steps. Given a single-electrode sEMG sequence of length N, a 2D Hilbert representation is achieved with dimensions M x M, where $N = M^2$ and M is a power of two, i.e. $M = 2^n$. If there are K sEMG electrodes, this process is repeated for every electrode, and the outputs are stacked into a K-channel image, i.e. an image with dimensions M x M x K. For example, a sEMG segment of 10 electrodes with 64 samples is mapped into an

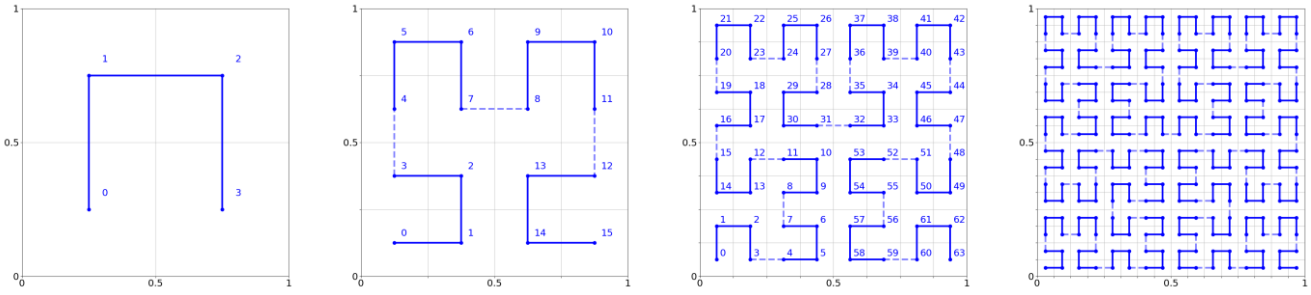

(a) (b) (c) (d)

Fig. 1. The first four iterations of the Hilbert curve.

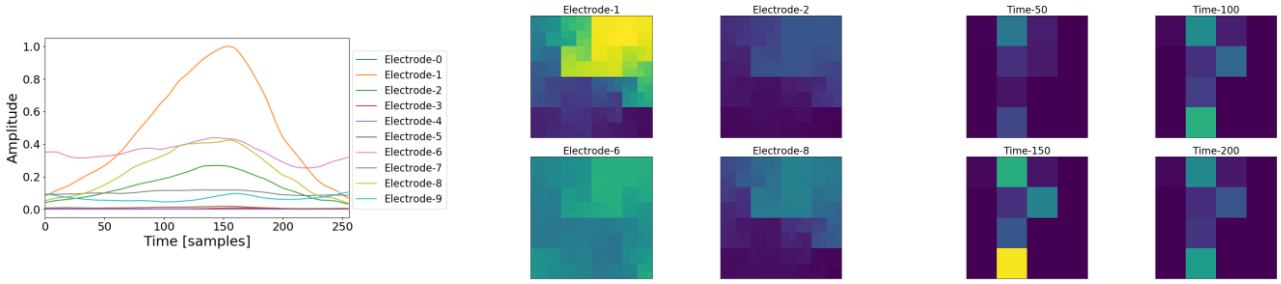

(a) (b) (c)

Fig. 2. The application of the Hilbert curve mapping to sEMG data. (a) A 256-samples segment of sEMG signal, (b) the Hilbert representation (16 x 16) across time of electrodes 1, 2, 6, 8, and (c) the Hilbert representation (4 x 4) across electrodes at time instants 50, 100, 150, 200. In (c) there are less electrodes than pixel dimensions, thus the last six pixels on the right of the images are zeros.

8 x 8 x 10 image. It is important to note that sequence segments of length smaller than M^2 can be used as well, however, in that case the final image will be either cropped or filled with zeros.

In the second case, the Hilbert mapping is applied across the sEMG electrodes. Specifically, the number of sEMG electrodes is a square number, i.e. $K = M^2$, where $M = 2^n$. The Hilbert mapping is applied at every time instant of the sequence resulting in an image with dimensions M x M x N. For example, a sEMG segment of 16 electrodes with 20 samples is mapped into a 4 x 4 x 20 image. As in the previous case, if the number of electrodes is less than M^2 the final image will be either cropped or filled with zeros.

C. Network architecture

Usually in image applications, CNNs receive as input images with one channel (grayscale) or three channels (RGB). In our approach, the image dimension corresponds either to the number of electrodes or the segment duration.

Apart from networks that have been previously applied to the problem of hand gesture recognition [34], we investigate the application of CNN architectures that are typically found in image tasks, such as VGGNet [31], DenseNet [17], and SqueezeNet [19]. To keep comparisons of the results fair, an effort is made to keep the number of trainable parameters of the networks equal. The model architectures are presented in Table I.

IV. Experiments

A. Dataset

The proposed method was evaluated on data from the first dataset of the Ninapro database [2]. It includes data acquisitions of 27 healthy subjects that repeat each of the 52 gestures 10 times. The types of gestures can be divided into three groups: i) basic finger movements, ii) isometric, isotonic hand configurations and basic wrist movements, and iii) grasping and functional movements. The data are acquired with 10 electrodes, of which eight are placed around the forearm and the other two are placed on the main activity spots of the large flexor and extensor muscles of the forearm [2].

The sEMG signals were preprocessed with a low-pass filter as in previous studies on Ninapro database [3, 14, 34]. Then, training data are augmented by duplicating the signals of each repetition and adding Gaussian noise with a signal to noise ratio (SNR) equal to 25dB. In addition, sEMG signals are augmented with the magnitude-warping method described in [36, 35]. As a last step, sEMG signals from the 10 channels are segmented into overlapping windows of length N with a step of 50ms and organized into N x 10 arrays.

B. No Hilbert (baseline)

As our baseline, we take the approach where the Hilbert mapping is not used. Therefore, the N x 10 arrays are fed into

TABLE I. CNN Model Architectures Used in This Work.

	AtzoriNet [3, 34]	**VGGNet [31]**	**DenseNet [17]**	**SqueezeNet [19]**
	CONV(32, 1x10), ReLU, CONV(32, 3x3), ReLU, POOL(max, 3x3), CONV(64, 5x5), ReLU, POOL(max, 3x3), CONV(64, 5x1), ReLU, CONV(G, 1x1), Softmax	CONV(16, 3x3), BN, ReLU, CONV(32, 3x3), ReLU, CONV(32, 3x3), ReLU, POOL(max, 2x2), CONV(64, 3x3), ReLU, CONV(64, 3x3), ReLU, POOL(max, 2x2), GLPOOL(avg), FC(G), Softmax	CONV(16, 3x3), BN, ReLU, DSBLOCK(4), TRBLOCK(50), DSBLOCK(3), TRBLOCK(75), ReLU, CONV(G, 1x1), ReLU, GLPOOL(avg), Softmax DSBLOCK(n) {BN, ReLU, CONV(16, 3x3)}$_n$ TRBLOCK(k) BN, CONV(k, 1x1), POOL(max)	CONV(16, 3x3), BN, ReLU, SQBLOCK(4, 16, 32), SQBLOCK(3, 16, 64), CONV(G, 1x1), ReLU, GLPOOL(avg), Softmax SQBLOCK(a, b, c) {FIRE(b, c)}$_a$, POOL(max) FIRE(b, c) CONV(b, 1x1), ReLU, CONV(c, 1x1), ReLU + CONV(c, 3x3), ReLU
Parameters	85K	75K	70K	70K

CONV: convolutional layer, POOL: pooling layer, GLPOOL: global pooling layer, FC: fully-connected layer, BN: batch normalization, {}$_k$: repetition k times, '+': concatenation
G: number of gesture labels

the CNN models as single-channel images. For the window length N, we experiment with two values: 15 and 64 samples using all the models in Table I.

C. Hilbert mapping across time dimension (HilbTime)

In the case of the Hilbert mapping across time dimension (HilbTime), the N x 10 segments are organized into M x M x10 images. For N values equal to 16 and 64 the resulting image sizes are 4 x 4 x 10 and 8 x 8 x 10 respectively. From Table I, only the VGG, Dense and Squeeze models were used.

D. Hilbert mapping across elextrode dimension (HilbElect)

The Hilbert mapping across sEMG channel dimension (HilbElect) is applied in a similar fashion. The N x 10 segments are organized into 4 x 4 x N images. In this approach we retain the spatial resolution constant due to the small number of available electrodes. In addition, the pixels that correspond to the last six positions the Hilbert curve traverses are set to zero. For the window length, we only experimented with N = 16, since this parameter does not affect the spatial resolution of the images. As in the previous case, only the VGG, Dense and Squeeze models were used.

E. Model hyper-parameters

All networks were trained using stochastic gradient descent for 60 epochs with initial learning rate of 0.1 halved every 15 epochs and a batch size of 1024. To avoid overfitting the networks due to the small training set, dropout layers were appended after each convolutional layer with a forget rate of 0.3. In addition, weight decay regularization with a value of 0.0005 was applied to all convolutional layers. These values were selected after performing a grid search on a validation set of ten randomly selected subjects.

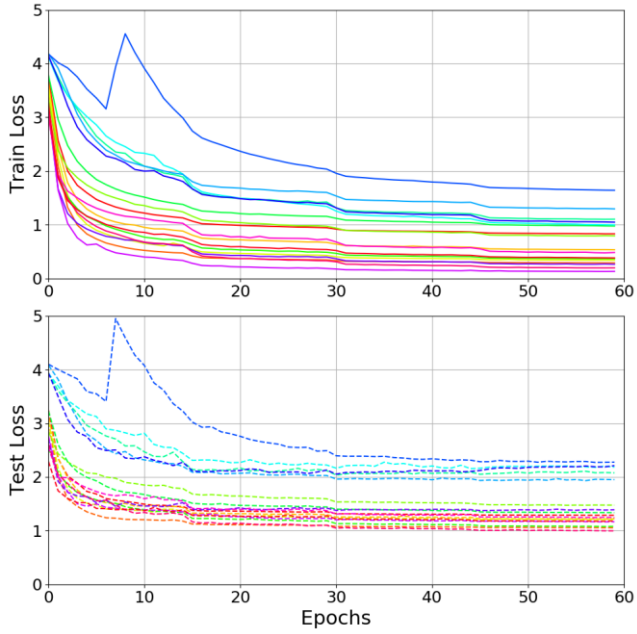

Fig. 3. Loss graphs on the train and test sets.

F. Evaluation

The evaluation is based on existing works that have used the Ninapro dataset [3, 14, 34]. Specifically, for each subject a new model is trained on data from seven repetitions and tested on the remaining three. As performance metrics we use the top-1 and top-3 accuracies (i.e. the accuracy when the highest and any of the 3 highest output probabilities match the expected gesture), as well as precision and recall values. For each metric, the average across the 27 subjects in the dataset is reported.

V. Results and Discussion

The problem of hand gesture recognition based on sEMG is addressed as an image classification task, where the Hilbert curve is utilized for the representation of sEMG signals as images. In the experiments, we investigate two ways of applying the Hilbert curve, which are evaluated across four CNN models. A comparison of the loss graphs during training and testing (Fig. 3) shows that all models have been trained until convergence. The results of the evaluation experiments are presented in Table II and Fig. 4.

From Fig. 4 we can see that using the Hilbert mapping the models perform equally well or even better compared to the corresponding baseline approach without the Hilbert representation. Compared to our previous results [34], the baselines for the VGG and the DenseNet yield similar results, while the Hilbert mappings are beneficial for these models. In addition, the VGG architecture performed the best between the counterpart models, while the SqueezeNet had always the poorest performance in every evaluation metric.

A comparison between the Hilbert mapping methods and the corresponding baseline for input segments of length N = {16,64} for the VGG, Dense and Squeeze models is performed with a Wilcoxon signed rank test at a 5% significance level. Specifically, the baseline with input 15 x 10 is compared to the HilbTime approach with input 4 x 4 x 10 and the HilbElect, while the HilbTime method with input 8 x 8 x 10 is compared to the 64 x 10 baseline. The results are shown in Table II where an '*' denotes a significant difference. We see that for the VGG model both Hilbert mapping approaches give superior results than the corresponding baselines (3.1% improvement for HilbTime and 3.5% for HilbElect). On the other hand, for the DenseNet model the Hilbert across time with N = 16 did not provide any improvement, while for N = 64 and the HilbElect mapping the results were better.

VI. Conclusions

This work investigated the utilization of the Hilbert curve as a means of representing sEMG signals as images in the problem of gesture recognition. Two approaches were evaluated: the application across the time dimension and across the electrodes dimension. In our experiments, we compared three CNN architectures that have been widely used in image tasks along with a model optimized for the problem of gesture recognition. The results showed that a VGG-based network had the best performance on a benchmark dataset. Finally, although the representation of sEMG signals with the Hilbert curve seems to improve the performance of CNN models, more experiments are needed before safe conclusions are reached.

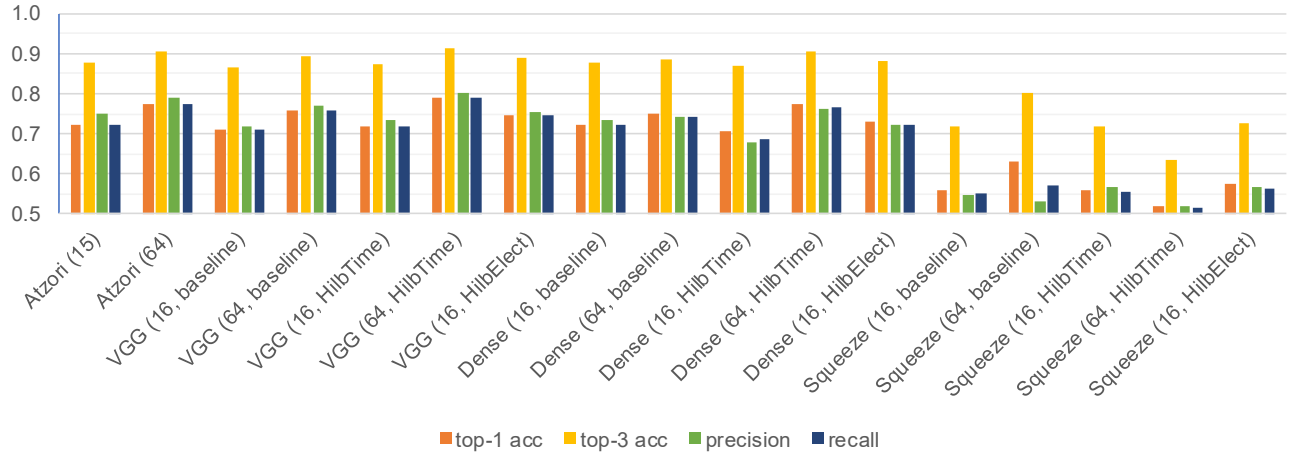

Fig. 4. Evaluation experiments results. The metrics are computed for the test set.

TABLE II. PERFORMANCE RESULTS.

	VGGNet [31]					DenseNet [17]					SqueezeNet [19]				
	16x10	**64x10**	**4x4x10**	**8x8x10**	**4x4x16**	**16x10**	**64x10**	**4x4x10**	**8x8x10**	**4x4x16**	**16x10**	**64x10**	**4x4x10**	**8x8x10**	**4x4x16**
top-1 accuracy	0.7115 (0.0682)	0.7592 (0.0626)	0.7192* (0.0670)	**0.7908*** (0.0570)	0.7469* (0.0653)	0.7225 (0.0639)	0.7493 (0.0648)	0.7064* (0.0634)	0.7757* (0.0588)	0.7319* (0.0598)	0.5611 (0.2342)	0.6297 (0.1445)	0.5585 (0.1995)	0.5188 (0.3298)	0.5742 (0.2144)
top-3 accuracy	0.8640 (0.0492)	0.8945 (0.0443)	0.8754* (0.0449)	**0.9156*** (0.0361)	0.8910* (0.0440)	0.8770 (0.0458)	0.8868 (0.0439)	0.8703* (0.0439)	0.9073* (0.0368)	0.8837* (0.0414)	0.7175 (0.2783)	0.8002 (0.1586)	0.7172 (0.2367)	0.6357 (0.3726)	0.7255 (0.2455)
precision	0.7174 (0.0676)	0.7702 (0.0633)	0.7334* (0.0622)	**0.8031*** (0.0559)	0.7562* (0.0632)	0.7326 (0.0634)	0.7412 (0.0663)	0.6785* (0.0669)	0.7637 (0.0663)	0.7237 (0.0603)	0.5461 (0.2392)	0.5319 (0.1721)	0.5687 (0.2115)	0.5189 (0.3473(	0.5671 (0.2195)
recall	0.7110 (0.0679)	0.7594 (0.0640)	0.7205* (0.0659)	**0.7904*** (0.0579)	0.7467* (0.0677)	0.7218 (0.0642)	0.7417 (0.0645)	0.6863* (0.0661)	0.7651 (0.0610)	0.7243 (0.0607)	0.5524 (0.2302)	0.5712 (0.1618)	0.5545 (0.1986)	0.5158 (0.3281)	0.5630 (0.2118)

values in parentheses correspond to standard deviation

ACKNOWLEDGMENTS

The work is supported by the «Andreas Mentzelopoulos Scholarships for the University of Patras» and the VUB-UPatras International Joint Research Group (IJRG) on ICT.

REFERENCES

[1] M. Atzori et al., "Building the Ninapro database: A resource for the biorobotics community," Proc. IEEE RAS EMBS Int. Conf. Biomed. Robot. Biomech., pp. 1258–1265, 2012.

[2] M. Atzori et al., "Electromyography data for non-invasive naturally-controlled robotic hand prostheses," Sci. Data, vol. 1, p. 140053, 2014.

[3] M. Atzori, M. Cognolato, and H. Müller, "Deep Learning with Convolutional Neural Networks applied to electromyography data: A resource for the classification of movements for prosthetic hands," Front. Neurorobot., vol. 10, Sep. 2016.

[4] J. H. Bappy, C. Simons, L. Nataraj, B. S. Manjunath, and A. K. Roy-Chowdhury, "Hybrid LSTM and Encoder-Decoder Architecture for Detection of Image Forgeries," IEEE Trans. Image Process., pp. 1–1, 2019.

[5] C. Castellini, A. E. Fiorilla, and G. Sandini, "Multisubject/daily-life activity EMG-based control of mechanical hands.," J. Neuroeng. Rehabil., vol. 6, p. 41, Nov. 2009.

[6] Y.-J. Chang, S.-F. Chen, and J.-D. Huang, "A Kinect-based system for physical rehabilitation: A pilot study for young adults with motor disabilities," Res. Dev. Disabil., vol. 32, no. 6, pp. 2566–2570, Nov. 2011.

[7] X. Chen et al., "Hand gesture recognition research based on surface EMG sensors and 2D-accelerometers," in 2007 11th IEEE Intern. Symp. on Wearable Computers, pp. 1–4, 2007.

[8] M. J. Cheok, Z. Omar, and M. H. Jaward, "A review of hand gesture and sign language recognition techniques," Int. J. Mach. Learn. Cybern., vol. 0, Aug. 2017.

[9] T. Corcoran, R. Zamora-Resendiz, X. Liu, and S. Crivelli, "A Spatial Mapping Algorithm with Applications in Deep Learning-Based Structure Classification," Feb. 2018.

[10] U. Côté-Allard et al., "Deep Learning for electromyographic hand gesture signal classification using Transfer Learning," ArXiv e-prints, Jan. 2018.

[11] S. Dhahbi, W. Barhoumi, J. Kurek, B. Swiderski, M. Kruk, and E. Zagrouba, "False-positive reduction in computer-aided mass detection using mammographic texture analysis and classification," Comput. Methods Programs Biomed., vol. 160, pp. 75–83, Jul. 2018.

[12] Y. Du et al., "Surface EMG-based inter-session gesture recognition enhanced by deep domain adaptation," Sensors, vol. 17, no. 3, p. 458, Feb. 2017.

[13] D. Farina et al., "The Extraction of Neural Information from the Surface EMG for the Control of Upper-Limb Prostheses: Emerging Avenues and Challenges," IEEE Trans. Neural Syst. Rehabil. Eng., vol. 22, no. 4, pp. 797–809, Jul. 2014.

[14] W. Geng et al., "Gesture recognition by instantaneous surface EMG images," Sci. Rep., vol. 6, no. 36571, 2016.

[15] A. Gijsberts et al., "Movement error rate for evaluation of Machine Learning methods for sEMG-based hand movement classification," IEEE Trans. Neural Syst. Rehabil. Eng., vol. 22, no. 4, pp. 735–744, Jul. 2014.

[16] C. Gotsman and M. Lindenbaum, "On the metric properties of discrete space-filling curves," IEEE Trans. Image Process., vol. 5, no. 5, pp. 794–797, May 1996.

[17] G. Huang, Z. Liu, L. van der Maaten, and K. Q. Weinberger, "Densely Connected Convolutional Networks," ArXiv e-prints, Aug. 2016.

[18] B. Hudgins, P. Parker, and R. N. Scott, "A new strategy for multifunction myoelectric control," IEEE Trans. Biomed. Eng., vol. 40, no. 1, pp. 82–94, 1993.

[19] F. N. Iandola, S. Han, M. W. Moskewicz, K. Ashraf, W. J. Dally, and K. Keutzer, "SqueezeNet: AlexNet-level accuracy with 50x fewer parameters and <0.5MB model size," ArXiv e-prints, Feb. 2016.

[20] S. Ioffe and C. Szegedy, "Batch Normalization: Accelerating deep network training by reducing internal covariate shift," ArXiv e-prints, Mar. 2015.

[21] N. Jiang et al., "Is accurate mapping of EMG signals on kinematics needed for precise online myoelectric control?," IEEE Trans. Neural Syst. Rehabil. Eng., vol. 22, no. 3, pp. 549–558, May 2014.

[22] J. Kurek, B. Swiderski, S. Osowski, M. Kruk, and W. Barhoumi, "Deep learning versus classical neural approach to mammogram recognition," Bull. Pol. Ac. Tech, vol. 66, no. 6, 2018.

[23] I. Kuzborskij, A. Gijsberts, and B. Caputo, "On the challenge of classifying 52 hand movements from surface electromyography," in 2012 Annual Intern. Conf. of the IEEE Engineering in Medicine and Biology Society, pp. 4931–4937, 2012.

[24] Y. Li et al., "Revisiting Batch Normalization for practical domain adaptation," ArXiv e-prints, Nov. 2016.

[25] B. Moon, H. V. Jagadish, C. Faloutsos, and J. H. Saltz, "Analysis of the clustering properties of the Hilbert space-filling curve," IEEE Trans. Knowl. Data Eng., vol. 13, no. 1, pp. 124–141, 2001.

[26] S. Muceli, N. Jiang, and D. Farina, "Extracting signals robust to electrode number and shift for online simultaneous and proportional myoelectric control by factorization algorithms," IEEE Trans. Neural Syst. Rehabil. Eng., vol. 22, no. 3, pp. 623–633, May 2014.

[27] L. Omelina et al., "Serious games for physical rehabilitation: designing highly configurable and adaptable games," in Proceedings of the 9th Intern. Conf. on Disability, Virtual Reality & Associated Technologies, pp. 195–201, 2012.

[28] K.-H. Park and S.-W. Lee, "Movement intention decoding based on Deep Learning for multiuser myoelectric interfaces," in 2016 4th Intern. Winter Conf. on BrainComputer Interface (BCI), pp. 1–2, 2016.

[29] S. S. Rautaray and A. Agrawal, "Vision based hand gesture recognition for human computer interaction: a survey," Artif. Intell. Rev., vol. 43, no. 1, pp. 1–54, Jan. 2015.

[30] E. Scheme and K. Englehart, "Electromyogram pattern recognition for control of powered upper-limb prostheses: State of the art and challenges for clinical use," J. Rehabil. Res. Dev., vol. 48, no. 6, p. 643, 2011.

[31] K. Simonyan and A. Zisserman, "Very deep convolutional networks for large- scale image recognition," in Proc. Int. Conf. Learning Representations, 2015.

[32] N. Srivastava et al., "Dropout: A simple way to prevent Neural Networks from overfitting," J. Mach. Learn. Res., vol. 15, pp. 1929–1958, 2014.

[33] A. Stango, F. Negro, and D. Farina, "Spatial correlation of high density EMG signals provides features robust to electrode number and shift in pattern recognition for myocontrol," IEEE Trans. Neural Syst. Rehabil. Eng., vol. 23, no. 2, pp. 189–198, Mar. 2015.

[34] P. Tsinganos et al., "Deep Learning in EMG-based Gesture Recognition," in Proceedings of the 5th Intern. Conf. on Physiological Computing Systems, pp. 107–114, 2018.

[35] P. Tsinganos, A. Skodras, B. Cornelis, and B. Jansen, "Deep Learning in Gesture Recognition Based on sEMG Signals," in Learning Approaches in Signal Processing, 1st ed., F. Ring, W.-C. Siu, L.-P. Chau, L. Wang, and T. Tang, Eds. Pan Stanford Publishing, 2018, p. 471.

[36] T. T. Um et al., "Data augmentation of wearable sensor data for parkinson's disease monitoring using convolutional neural networks," in Proceedings of the 19th ACM International Conference on Multimodal Interaction - ICMI 2017, 2017, vol. 517, pp. 216–220.

[37] W. Wei et al., "A multi-stream Convolutional Neural Network for sEMG-based gesture recognition in musclecomputer interface," Pattern Recognit. Lett., Dec. 2017.

[38] B. Yin, M. Balvert, D. Zambrano, A. Schönhuth, and S. Bohte, "An image representation based convolutional network for DNA classification," ArXiv e-prints, Jun. 2018.